Interfacial activity of nitric acid at the water–supercritical CO_2 interface: a molecular dynamics investigation

Rachel Schurhammer and Georges Wipff*

Laboratoire MSM (CNRS UMR 7551), Institut de Chimie, Université Louis Pasteur, 4, rue B. Pascal, 67000 Strasbourg, France. E-mail: wipff@chimie.u-strasbg.fr

Received (in Montpellier, France) 23rd July 2001, Accepted 9th October 2001
First published as an Advance Article on the web

We report a molecular dynamics study on a nitric acid water–supercritical CO_2 interface. Three extreme models are compared, where the acid is either all neutral HNO_3, completely dissociated into NO_3^- and H_3O^+, or represented by a 1 : 1 mixture of both forms. The ionic species are found to be "repelled" by the neat interface, while the neutral HNO_3 molecules are highly surface active. Similar features are observed with SC-CO_2 or with chloroform as the organic phase, pointing to the generality of interfacial activity of the acid.

Solvation at liquid–liquid interfaces (LLI) between two immiscible liquids displays peculiar properties[1] compared to pure liquid phases, as revealed by microscopic pictures emerging from Monte Carlo[2,3] or molecular dynamics (MD)[4,5] simulations. This paper deals with the distribution of nitric acid at an aqueous LLI. Acidic LLI's are important in the context of electrochemical processes,[6] as mimics of membrane aqueous interfaces,[7] as well as in the context of liquid–liquid ion extraction from an acidic aqueous phase to an organic phase.[8] For instance, nuclear waste partitioning in the PUREX process starts after dissolution of solid irradiated material in an aqueous nitric acid solution.[9] It is stressed that acidity modifies the properties of the interface, be it neat or covered by amphiphilic molecules, as indicated by surface tension measurements on the benzene–tri-n-butylphosphate–aqueous nitric acid system.[10] There are also analogies between the LLI and the water–air interface, onto which polar species such as acids[11–13] or phenols[14,15] adsorb. There are, however, no microscopic pictures of the distribution of the acid at the interface. This led us to recently simulate a nitric acid water–"oil" interface, where the oil was modelled by chloroform.[16] Here, we consider supercritical CO_2 (SC-CO_2) as the organic medium. SC-CO_2 represents a promising alternative in solvent extraction, compared to classical solvents, as it is less polluting and can be easily separated from the extraction system.[17] MD investigations on a pH-neutral water–SC-CO_2 interface[18] showed that it displays similarities with the water–chloroform interface, onto which extractant molecules like alkylphosphates or calixarenes adsorb. The investigations of nitric acid at the water–SC-CO_2 interface represent a first step before the modeling of more complex heterogeneous systems.

As bond-making and -breaking processes cannot be modelled satifactorily in the force field representation of the potential energy used in classical MD simulations, an *a priori* choice has to be made concerning the status of the proton. We therefore considered two extreme models of the acid, referred to below as "neutral" (HNO_3 form) and "ionic" (dissociated NO_3^- and H_3O^+ ions). The neutral model is not realistic in aqueous conditions, but more likely represents the acid extracted into an organic medium of low polarity. The ionic model is more adequate in water solution, although the proton might also be involved in $H_5O_2^+$ species or in higher water aggregates. We thus considered concentrated solutions of HNO_3 alone (system **A**), of NO_3^- and H_3O^+ alone (system **B**), and 1 : 1 mixtures of both (**C** and **D**). In **A**–**C**, the total aqueous acid concentration is about 1 mol L^{-1}, while in **D**, it is about 1.6 mol L^{-1}.

Methods

The MD simulations were performed with the AMBER5.0 software[19] in which the potential energy is described by a sum of bond, angle and dihedral deformation energies, and pairwise additive 1-6-12 (electrostatic + van der Waals) interactions between non-bonded atoms:

$$U = \Sigma_{\text{bonds}} K_r (r - r_{\text{eq}})^2 + \Sigma_{\text{angles}} K_\theta (\theta - \theta_{\text{eq}})^2 + \Sigma_{\text{dihedrals}} \Sigma_n V_n (1 + \cos n\phi) + \Sigma_{i<j} [q_i q_j / R_{ij} - 2\varepsilon_{ij} (R_{ij}^*/R_{ij})^6 + \varepsilon_{ij} (R_{ij}^*/R_{ij})^{12}]$$

The charges of the solute species were the same as in ref. 16: $q_N = 0.968$, $q_O = -0.526$ and $q_H = 0.464$ for HNO_3, $q_O = -0.620$ and $q_H = 0.540$ for H_3O^+ and $q_N = 0.905$, $q_O = -0.635$ e for NO_3^-. Water was represented with the TIP3P model[20] and CO_2 by the three-site model of Murthy *et al.*[21]: charges $q_C = 0.596$, $q_O = -0.298$ e and van der Waals parameters $R^*_O = 1.692$, $R^*_C = 1.563$ Å and $\varepsilon_O = 0.165$, $\varepsilon_C = 0.058$ kcal mol^{-1}.

The interface has been built as indicated in ref. 22, starting with two adjacent boxes of pure water and CO_2, respectively (Fig. 1). Aggregates of the acid molecules were first optimized in the gas phase and immersed in the aqueous phase, within the cutoff distance from the interface. All systems were represented with 3D periodic boundary conditions, corresponding therefore to alternating slabs of water and CO_2. The non-bonded interactions were calculated with a residue-based 12/15 Å twin cutoff and a reaction field (RF) correction for the electrostatics.[23] The RF assumes that the charge distribution of a sphere of cutoff radius interacts with a polarizable continuum dielectric medium, and prevents discontinuities of the energy at the cutoff boundaries, especially in systems with high concentrations of charges. We preferred to use the RF rather the 3D Ewald summation corrections of the electrostatics, because of the less symmetrical nature of the 2D interface.

The initial density of the CO_2 box was 0.80 g cm^{-3}, which is above the critical density (0.47 g cm^{-3} at 304 K) and close to the density of 0.79 g cm^{-3} at 345 K and a pressure of 30 MPa.[24]

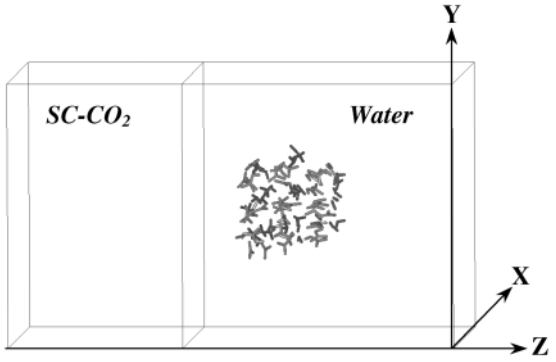

Fig. 1 Schematic representation of the simulation box with the initial arrangement of the 18 (H_3O^+, NO_3^-) acid species (0 ps).

Although it would be desirable to run the simulations at constant pressure this procedure turned out to be difficult due to the high fluctuations and problems associated with correctly monitoring the pressure of both phases. This is why we decided to perform the simulations at constant volume, starting with a density of 1.0 g cm^{-3} for water and 0.80 g cm^{-3} for CO_2. All solvent bonds were constrained with SHAKE, using a time step of 2 fs. After energy minimization, the dynamics was run for 1 ns at 350 K, independently coupling the water, CO_2 and acid subsystems to a thermal bath using the Berendsen algorithm,[25] with a relaxation time of 0.2 ps. The characteristics of the simulated systems are given in Table 1.

The results were analyzed as described in refs. 22 and 26. The position of the interface was recalculated every 0.2 ps, as the intersection between the water and CO_2 density curves. The distribution of NO_3^-, H_3O^+ or HNO_3 species was characterized by the corresponding density curves (Fig. 2; averages taken during the last 0.2 ns). The average relative populations (%) of these species found within 7 Å of the interface (this distance is about half of the interfacial width) were also calculated (Table 2). Their fluctuations were about 3%. There is no unique definition of the interfacial thickness. It can be characterized by the density curves (*e.g.*, corresponding decay from about 95% to 5%). Here, the instantaneous interfacial thickness e was defined as in refs 27 and 28 by the difference of the positions of interfacial water molecules, $z_{max}(t)-z_{min}(t)$, at each time t. The corresponding average $\langle e \rangle$ and fluctuations were obtained during the last 200 ps.

Results

Acid distribution near the interface

Typical snapshots at the end of the dynamics and average density curves of the solvents and acid along the Z direction are given in Fig. 2. With the two models of nitric acid, the water and CO_2 liquids remain more or less separated by an interface, as in the pH-neutral biphasic system,[18] but the acidic interface is rougher. As the systems have been simulated with 3D-periodicity, there are thus in fact two water–CO_2 interfaces. With all acid models also, most of the acid sits in water, while the CO_2 bulk phase is "pure". It contains practically no acid, nor water molecules. This contrasts with the water phase where some CO_2 molecules are dissolved during the dynamics. There is, however, a marked difference in the acid distribution, depending on the model used.

With the neutral model (system **A**), there is a pronounced peak of HNO_3 molecules at the interface, which decreases steeply on the CO_2 side and less so on the water side: on average, 34% of the neutral acid sits within 7 Å of the interface where HNO_3 molecules are hydrogen-bonded to water molecules *via* their NO–H proton. The O_{NO3} oxygens form fewer hydrogen bonds at the interface. This distribution markedly differs from the one observed with the fully ionic model (system **B**) with H_3O^+ and NO_3^- species diluted in bulk water. Only 10% of these ions are found within 7 Å of the interface, as a result of the larger hydrophilicity, compared to HNO_3.

When 1 : 1 mixtures of neutral and ionic forms (systems **C** and **D**) are simulated under the same conditions, one finds the main features of their components. The HNO_3 species display a peak of concentration at the nearest interface, as in the all-neutral model system **A**, while the ionic NO_3^- and H_3O^+ species are "repelled" by the interface and diluted in the bulk water phase, hydrogen-bonded to the surrounding water molecules. There is no difference in the cation *vs.* anion distribution near the interface, where the corresponding density curves are nearly superposed. Only 6% of each of these species sit within 7 Å of the interface. This contrasts with the patterns found under standard conditions at the water–chloroform interface,[16] where interfacial HNO_3 molecules were hydrogen-bonded to NO_3^- anions, enhancing therefore their concentration near the interface. This difference is likely due to the higher temperature and pressure in the supercritical systems **C** and **D**. As a result, the interfacial HNO_3 molecules are more randomly oriented, leading, on the average, to a zero dipole moment along the z direction. In these systems, there are no $NO_3^- \cdots H_3O^+$ ion pairs either, likely because the ions are preferentially hydrated.

Interestingly, as the acid concentration is increased by a factor 1.6 (compare systems **C** and **D**) the proportion of interfacial HNO_3 molecules increases (from 26% to 40%) while the proportion of NO_3^- and H_3O^+ ions remains constant (6%). This should lead to a decrease in interfacial pressure, consistent with experimental measurements.[29] This is an important feature in the context of ion extraction from aqueous media of high acidity, as the interface crossing by complexed ions is facilitated by the high acid concentration.

Shape of the interface

It can be seen from the water and CO_2 density curves that the interface is of about 15 Å width on the average. However, instantaneous pictures (*e.g.*, at 1 ns, Fig. 3) reveal that the solvent surfaces are not flat. They look rougher than with chloroform as the organic phase simulated under standard conditions.[27] There is no systematic trend or correlation between surface roughness and nature of the solute, as in the ionic system **B**; there is no acid at the interface, but the latter is also very rough, while in the other systems one generally finds HNO_3 species at the surface of water protuberances.

Table 1 Simulation conditions: number of solvent molecules and box sizes $[X \times Y \times (Z_{CO_2}+Z_{wat})]$.

System		Time/ns	Box size/Å^3	CO_2 molecules	H_2O molecules	Acid conc./mol L^{-1}
A	36 HNO_3	1	$43 \times 36 \times (23+38)$	408	1865	1.0
B	36 (H_3O^+, NO_3^-)	1	$43 \times 36 \times (23+38)$	409	1843	1.0
C	18 (HNO_3, H_3O^+, NO_3^-)	1	$43 \times 36 \times (23+38)$	409	1802	1.0
D	36 (HNO_3, H_3O^+, NO_3^-)	1	$44 \times 56 \times (31+31)$	813	2450	1.6

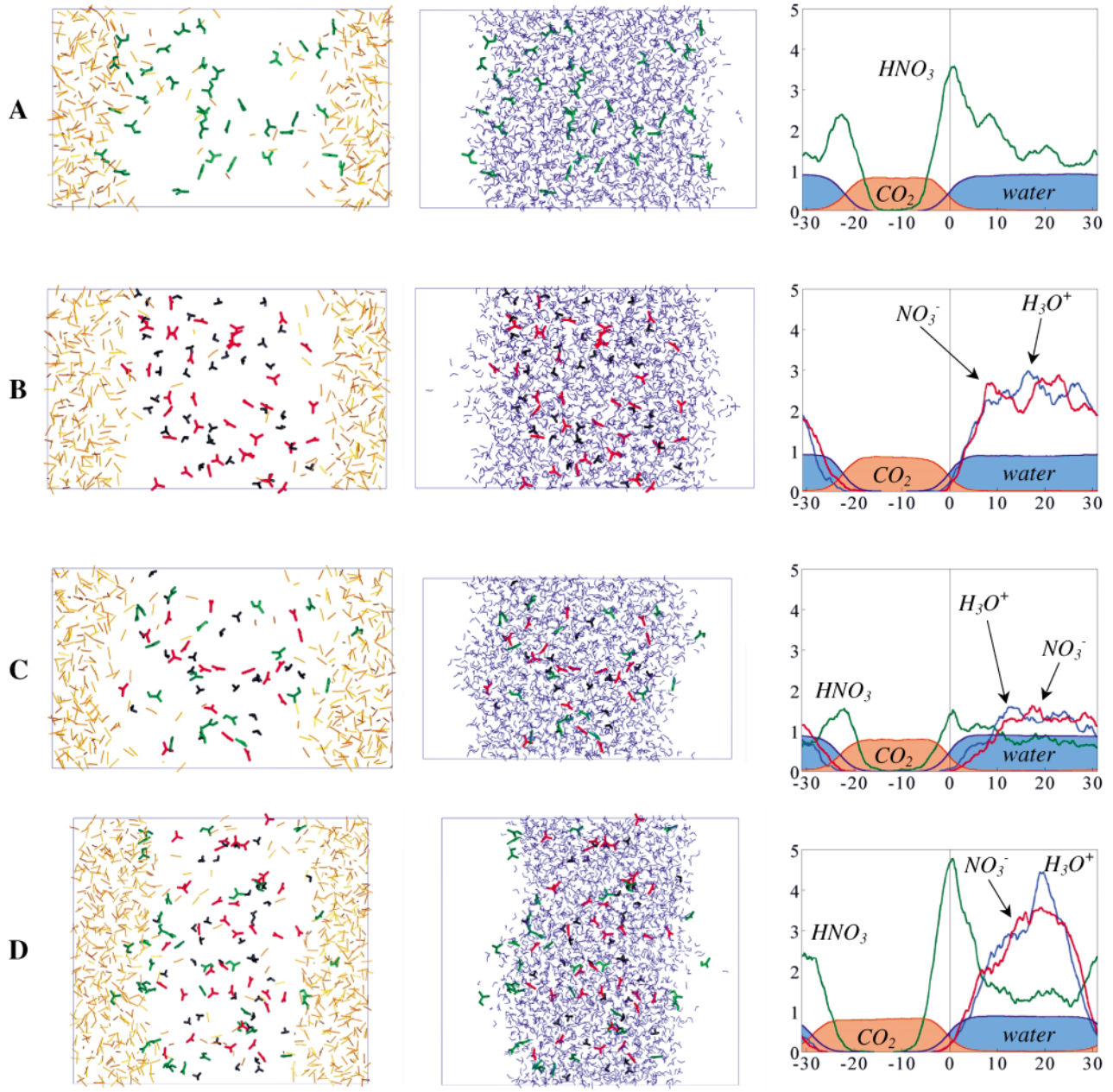

Fig. 2 The nitric acid water –SC-CO_2 interface at 1 ns. From top to bottom: neutral model **A**, 36 HNO_3; ionic model **B**, 36 (NO_3^-, H_3O^+); mixed model **C**, 18 (HNO_3, NO_3^-, H_3O^+); mixed model **D**: 36 (HNO_3, NO_3^-, H_3O^+). Right: density profiles of the solvents and solutes, calculated during the last 0.2 ns.

The water surface is displayed in Fig. 3, showing its roughness. The extrema dynamically exchange during the simulation, facilitating therefore the exchange between the water and CO_2 phases. To characterize the roughness, we calculated the ratio R between the corresponding water area S_{wat} and the xy area (the axes are defined in Fig. 1). R is fairly constant (Table 3) and ranges from 2.3 in systems **B**–**D** to 2.4 in **A**, which is larger than the typical values of 1.6 obtained at water–chloroform interfaces in standard conditions.[28] We also calculated the average interfacial thickness $\langle e \rangle$. Again, $\langle e \rangle$ is fairly constant (Table 3) and ranges from 15.6 to 16.8 Å, which is also larger than at water–chloroform interfaces,[28] in accordance with the higher mobility of solvent molecules in the water–SC-CO_2 biphasic system. Note also the corresponding high fluctuations of $\langle e \rangle$ (about 2 Å).

Table 2 Percentage of species within 7 Å of the interface

System		% HNO_3	% H_3O^+	% NO_3^-
A	36 HNO_3	34	—	—
B	36 (H_3O^+, NO_3^-)	—	10	11
C	18 (HNO_3, H_3O^+, NO_3^-)	26	7	5
D	36 (HNO_3, H_3O^+, NO_3^-)	40	6	6

Discussion and conclusion

Molecular dynamics simulations reveal the activity of the neutral form of nitric acid at the water–C–CO_2 interface. This feature is similar to the one observed with chloroform as the organic liquid.[16] To our knowledge, there are no related experimental data at the aqueous interface with SC-CO_2, but our finding is consistent with recent experimental results concerning acids at the water–air interface, which bears some analogies with the simulated system. Surface tension,[29] sum

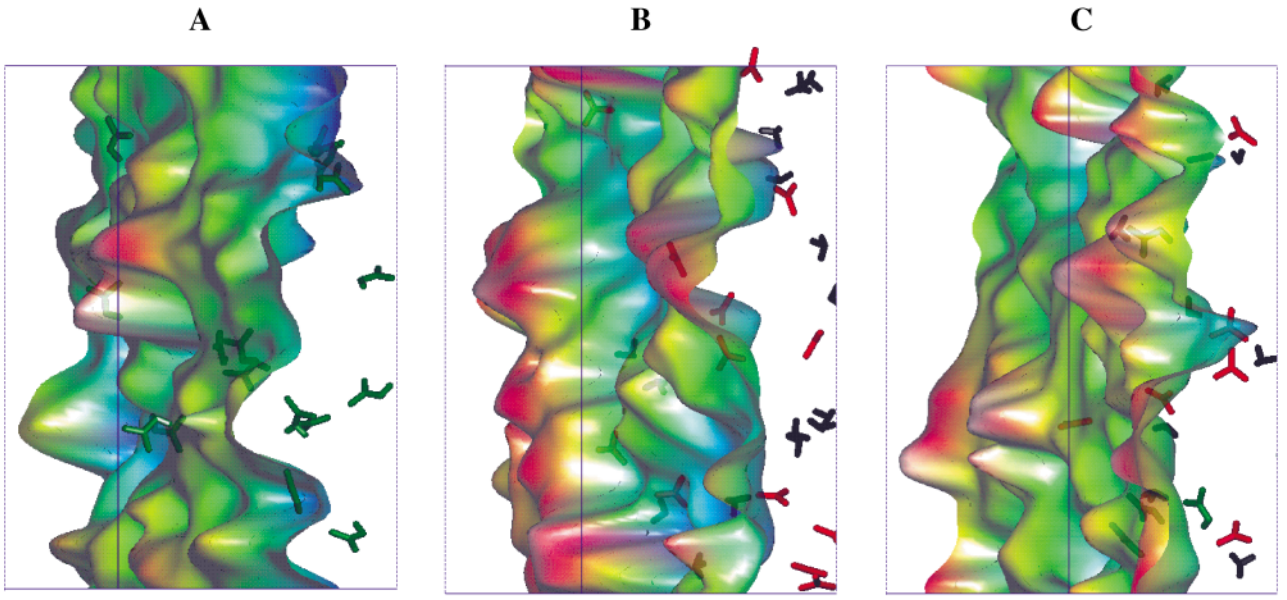

Fig. 3 Surface of water at the CO_2 interface, after 1 ns of MD in systems **A**, **B**, **C**. The water molecules (right-hand side of the surface) and CO_2 molecules (left-hand side of the surface) are not represented.

Table 3 Characteristics of the water–SC–CO_2 interface. Thickness $\langle e \rangle$, water area $\langle S_{wat} \rangle$ and $R = S_{wat}/xy$ ratio

System		$\langle e \rangle$/Å	$\langle S_{wat} \rangle$/Å^2	R
	No solute	14.3 ± 2.5	1877 ± 280	2.4
A	36 HNO_3	16.2 ± 1.9	3742 ± 323	2.4
B	36 (H_3O^+, NO_3^-)	15.9 ± 2.5	3561 ± 350	2.3
C	18 (HNO_3, H_3O^+, NO_3^-)	15.6 ± 2.1	3593 ± 300	2.3
D	36 (HNO_3, H_3O^+, NO_3^-)	16.8 ± 1.9	5761 ± 371	2.3

frequency,[12] molecular scattering measurements and surface proton exchange experiments[30] indeed suggest that HNO_3 is present at the surface of concentrated HNO_3–H_2O and ternary HNO_3–H_2SO_4–H_2O solutions.[31] From a mechanistic point of view, as far as ion extraction is concerned, it is generally observed that acid competes with metal extraction by ionophores.[32,33] This requires that the acid be able to easily cross the interface, and to have a non-negligible concentration in this mixed solvent border. Noteworthy in our calculations is the absence of acid in the CO_2 phase. This is also consistent with the fact that acid extraction is promoted *via* hydrogen-bonding interactions to the basic binding sites of extractant molecules.

Concerning the computations, a number of issues have been addressed in our previous studies on water–chloroform interfaces. Although solvent parameters fitted on pure liquids may inaccurately describe their mutual interactions,[34] we showed that several solvent models, some of them including explicit polarization terms, lead to similar results in demixing simulations.[35] The TIP3P model of water also leads to similar interfacial features as the more recently developed TIP5P model.[28] However, such water models overestimate the water polarity at hydrophobic surfaces[36] and therefore likely lead to exaggerated concentrations of ionic species at the water surface. Better models should account for the permanent dipole moment of water in the gas phase, as well as for the induced dipole moment in the bulk liquid.[37] Models with explicit polarization may lead to enhanced anion concentration, relative to cations, near the water surface.[38] Polarization may also have a subtle influence on the form taken by the proton (*e.g.*, H_3O^+ *versus* $H_5O_2^+$) near the interface, and also enhance the concentration of the neutral form HNO_3 of the acid, compared to the ionic forms.

Concerning the CO_2 representation, one can assume that the simple model we used depicts, at least qualitatively, the main features of the biphasic system. The representation of the system boundaries (2D *vs.* 3D) has also little effect on the interfacial properties.[35] Most critical is the representation of acidity, which represents a challenging task.[39] The best models should allow for proton transfer between the acid, water, or other bases,[40–42] as can be accounted for in principle by mixed MM/QM[39,43] or *ab initio* quantum dynamics treatments.[44–47] The acid should be neutral in the organic phase and dissociated in bulk water, but its pK_a near the interface is unknown. This critically determines the interfacial behavior, as shown in our study based on extreme model representations. We did not systematically explore concentration effects, which also determine the interfacial activity.

The most noticeable result, according to which the neutral form of the acid concentrates at the water–CO_2 and water–chloroform[16] interfaces, is consistent with pictures inferred from experiments at the water–air interface, and point to the importance of interfacial phenomena in acidic aqueous interfaces with supercritical fluids. *A fortiori*, other acids, which are more amphiphilic (*e.g.*, carboxylic acids) or more hydrophobic (*e.g.*, picric or perchloric acids) than HNO_3, should also concentrate at such interfaces.

Acknowledgements

The authors are grateful to CNRS-IDRIS and to Université Louis Pasteur for allocation of computer resources, to COST-D9 and to EEC (FIKW-CT2000-0088) for support. RS thanks the French Ministry of Research for a grant.

References

1 A. W. Adamson, *Physical Chemistry of Surfaces*, Wiley, New York 5th edn., 1990.
2 J. Gao and W. L. Jorgensen, *J. Phys. Chem.*, 1988, **92**, 5813–5822.
3 G. M. Torrie and J. P. Valleau, *J. Chem. Phys.*, 1980, **73**, 5807–5816.

4 I. Benjamin, *Annu. Rev. Phys. Chem.*, 1997, **48**, 407–451 and references cited therein.
5 F. Berny, N. Muzet, L. Troxler and G. Wipff, in *Supramolecular Science: Where It Is and Where It Is Going*, eds. R. Ungaro and E. Dalcanale, Kluwer Academic Pub., Dordrecht, 1999, pp. 95–125 and references cited therein.
6 H. H. Girault and D. J. Schiffrin, in *Electroanalytical Chemistry*, ed. A. J. Bard, Dekker, New York, 1989, pp. 1–141 and references cited therein.
7 A. G. Volkov, D. W. Deamer, D. L. Tanelian and V. S. Markin, *Liquid Interfaces in Chemistry and Biology*, John Wiley & Sons Inc., New York, 1998.
8 H. Watarai, *Trends Anal. Chem.*, **12**, 313–318.
9 L. Cecille, M. Casarci and L. Pietrelli, *New Separation Chemistry Techniques for Radioactive Waste and other Specific Applications*, Commission of the European Communities, Elsevier Applied Science, L ondon and New York, 1991.
10 E. Chifu, Z. Andrei and M. Tomoaia, *Anal. Chim. (Rome)*, 1974, **64**, 869–871.
11 S. Baldelli, C. Schnitzer, M. J. Shultz and D. J. Campbell, *J. Phys. Chem. B*, 1997, **101**, 10 435–10 441.
12 C. Schnitzer, S. Baldelli, D. J. Campbell and M. J. Shultz, *J. Phys. Chem.*, 1999, **103**, 6383–6386.
13 C. Schnitzer, S. Baldelli and M. J. Shultz, *J. Phys. Chem. B*, 2000, **104**, 585–590.
14 K. B. Eisenthal, *Chem. Rev.*, 1996, **96**, 1343–1360.
15 A. A. Tamburello-Luca, P. Hébert, P. F. Brevet and H. G. Girault, *J. Chem. Soc., Faraday Trans.*, 1996, **92**, 3079–3085.
16 M. Baaden, F. Berny and G. Wipff, *J. Mol. Liq.*, 2001, **90**, 3–12.
17 C. M. Wai and S. Wang, *J. Chromatogr., A*, 1997, **785**, 369–383.
18 R. Schurhammer, F. Berny and G. Wipff, *Phys. Chem. Chem. Phys.*, 2001, **3**, 647–656.
19 D. A. Case, D. A. Pearlman, J. C. Caldwell, T. E. Cheatham III, W. S. Ross, C. L. Simmerling, T. A. Darden, K. M. Merz, R. V. Stanton, A. L. Cheng, J. J. Vincent, M. Crowley, D. M. Ferguson, R. J. Radmer, G. L. Seibel, U. C. Singh, P. K. Weiner and P. A. Kollman, AMBER5, University of California, San Francisco, 1997.
20 W. L. Jorgensen, J. Chandrasekhar and J. D. Madura, *J. Chem. Phys.*, 1983, **79**, 926–936.
21 C. S. Murthy, K. Singer and I. R. McDonald, *Mol. Phys.*, 1981, **44**, 135–143.
22 M. Lauterbach, E. Engler, N. Muzet, L. Troxler and G. Wipff, *J. Phys. Chem. B*, 1998, **102**, 225–256.
23 P. H. Hünenberger and W. F. van Gunsteren, *J. Phys. Chem.*, 1998, **108**, 6117–6134.
24 B. F. Graham, A. F. Lagalante, T. J. Bruno, J. M. Harrowfield and R. D. Trengove, *Fluid Phase Equilib.*, 1998, **150–151**, 829–838.
25 H. J. C. Berendsen, J. P. M. Postma, W. F. van Gunsteren and A. DiNola, *J. Chem. Phys.*, 1984, **81**, 3684–3690.
26 G. Wipff, E. Engler, P. Guilbaud, M. Lauterbach, L. Troxler and A. Varnek, *New J. Chem.*, 1996, **20**, 403–417.
27 F. Berny, R. Schurhammer and G. Wipff, *Inorg. Chim. Acta*, 2000, **300–302**, 384–394.
28 R. Schurhammer, E. Engler and G. Wipff, *J. Phys. Chem.*, 2001, **105**, in press.
29 D. J. Donaldson and D. Anderson, *Geophys. Res. Lett.*, 1999, **26**, 3625.
30 J. Morris, P. Behr, M. D. Antman, B. R. Ringeisen, J. Splan and G. M. Nathanson, *J. Phys. Chem. A*, 2000, **104**, 6738.
31 H. Yang and B. J. Finlayson-Pitts, *J. Phys. Chem. A*, 2001, **105**, 1890–1896.
32 G. R. Choppin and K. L. Nash, *Radiochim. Acta*, 1995, **70–71**, 225–236.
33 P. R. Danesi, R. Chirizia and C. F. Coleman, in *Critical Reviews in Analytical Chemistry*, ed. B. Campbell, CRC Press, Boca Raton, FL, 1980, p. 1.
34 P. E. Smith and W. F. van Gunsteren, in *Computer Simulations of Biomolecular Systems*, eds. W. F. van Gunsteren, P. K. Weiner and A. J. Wilkinson, ESCOM, Leiden, 1993, pp. 182–212.
35 M. Lauterbach and G. Wipff, in *Physical Supramolecular Chemistry*, eds. L. Echegoyan and A. Kaifer, Kluwer Academic Pub., Dordrecht, 1996, pp. 65–102.
36 V. P. Sokhan and D. J. Tildesley, *Faraday Discuss.*, 1996, **104**, 193–208.
37 L. X. Dang and T. Chang, *J. Chem. Phys.*, 1997, **106**, 8149–8159.
38 E. M. Knipping, M. J. Lakin, K. L. Foster, P. Jungwirth, D. J. Tobias, R. B. Gerber, D. Dabdub and B. J. Finlayson-Pitts, *Science*, 2000, **288**, 301–306.
39 J. Gao, N. Li and M. Freindorf, *J. Am. Chem. Soc.*, 1996, **118**, 4912–4913.
40 R. G. Schmidt and J. Brickmann, *Ber. Bunsen-Ges. Phys. Chem.*, 1997, 1816–1827.
41 H. Sato and F. Hirata, *J. Phys. Chem. B*, 1999, **103**, 6596–6604.
42 S. R. Billeter and W. F. van Gunsteren, *J. Phys. Chem. A.*, 2000, **104**, 3276–3286.
43 K. Ando and J. T. Hynes, *J. Phys. Chem. A*, 1999, **103**, 10 398–10 408.
44 K. E. Laasonen and M. L. Klein, *J. Phys. Chem. A*, 1997, **101**, 98–102.
45 H. S. Mei, M. E. Tuckerman, D. E. Sagnella and M. L. Klein, *J. Phys. Chem. B*, 1998, **102**, 10 446–10 458.
46 D. M. Sullivan, K. Bagchi, M. E. Tuckerman and M. L. Klein, *J. Phys. Chem. A*, 1999, **103**, 8678–8683.
47 D. Marx, M. E. Tuckerman, J. Hutter and M. Parrinello, *Nature (London)*, 1999, **397**, 601–604.